

Structure and Dynamics of Disordered Tetrablock Copolymers: Composition and Temperature Dependence of Local Friction

Bryan R. Chapman,[‡] Mark W. Hamersky,[‡] Jodi M. Milhaupt,[†]
Clayton Kostecky,^{‡,§} and Timothy P. Lodge^{*,†}

Department of Chemistry and Department of Chemical Engineering & Materials Science, University of Minnesota, Minneapolis, Minnesota 55455

Ernst D. von Meerwall

Department of Physics and Maurice Morton Institute of Polymer Science, University of Akron, Akron, Ohio 44325

Steven D. Smith

The Procter & Gamble Company, Miami Valley Laboratories, Cincinnati, Ohio 45247

Received December 9, 1997

ABSTRACT: The structure factor, viscosity, and diffusivity of four (styrene-*b*-isoprene-*b*-styrene-*b*-isoprene) tetrablock copolymers have been examined as functions of temperature (T). The copolymers have styrene compositions (f) of 23, 42, 60, and 80 vol % and total degrees of polymerization ca. 120; polystyrene and polyisoprene homopolymers with similar degrees of polymerization have been used for comparison. Small angle neutron scattering (SANS) measurements in the disordered state are well-described by the appropriate Leibler/RPA structure factors, and extrapolation of the inverse peak intensities to lower T yields estimates of the order–disorder transition temperatures, which are at or below -50 °C. Consequently, over the T range of interest (25–180 °C) and over length scales greater than the chain dimensions, the tetrablocks provide homogeneous matrices containing varying amounts of styrene and isoprene, in which the f and T dependence of segmental friction may be examined. The diffusivity (determined by pulsed-field-gradient NMR and forced Rayleigh scattering) and viscosity provide estimates of the effective monomeric friction factor $\zeta_{\text{eff}}(f, T)$ via the Rouse model; the two dynamic properties yield equivalent values of ζ_{eff} . The T dependence of ζ_{eff} is well-described by the WLF function, with the f dependence almost entirely contained in the composition dependence of the glass transition temperature (T_g). Thus, when compared at constant $T - T_g$, $\zeta_{\text{eff}}(f)$ is only slightly larger than ζ_{PS}° or ζ_{PI}° , in marked contrast to the results for miscible blends such as PS/PVME and PS/PPO. Prediction of $\zeta_{\text{eff}}(f, T)$ on the basis of the homopolymer values alone, i.e., $\zeta_{\text{PS}}^\circ(T)$ and $\zeta_{\text{PI}}^\circ(T)$, is only successful when $T_g(f)$ is incorporated explicitly. An approach using equation of state estimates of free volume is significantly less successful, implying that the most important determinant of local friction in the mixture is the effective T_g sensed by each chain; $T_g(f)$ does not represent an iso-free volume state.

Introduction

Any dynamic property of a flexible polymer melt, such as the zero-shear-rate viscosity (η), dynamic shear modulus (G^*), or diffusion coefficient (D), can be written as the product of a universal function depending on molecular weight (M) and chain architecture and a monomer-specific function that primarily reflects an underlying characteristic segmental relaxation time.¹ These segmental dynamics are typically parametrized through the monomeric friction factor, ζ , and the strong temperature (T) dependence of ζ largely determines the T dependence of η , G^* , and D . For most polymers above their glass transition temperature (T_g), $\zeta(T)$ follows the Vogel–Fulcher or Williams–Landel–Ferry (WLF) form, although at a given $T - T_g$ the magnitude of ζ is still dependent on the identity of the monomer.² Thus for a single component polymer system, measurements of the T dependence of one dynamic quantity for a single M

are sufficient to estimate the T dependence of all dynamic properties for any M (except for chain end corrections at low M). In multicomponent systems, however, ζ of each component acquires a composition dependence about which very little is known. Consequently, it is generally impossible to predict the magnitude of a given dynamic quantity of a mixture solely on the basis of measurements on the individual components. Yet, quantitative predictions for important processes such as spinodal decomposition or blend compatibilization by added copolymers will require knowledge of the rate at which polymer A moves in a B-rich environment and vice versa.

Some progress has been made in monitoring $\zeta_A(\phi, T)$ and $\zeta_B(\phi, T)$ in *miscible* A/B blends, where ϕ is the volume fraction of component A, by measuring the tracer diffusion of each component in the mixture. The results are remarkable. For example, in polystyrene/polyphenyleneoxide (PS/PPO), ζ_{PS} is not a monotonic function of ϕ , even after accounting for the composition dependence of T_g .³ Furthermore, the ratio $\zeta_{\text{PS}}/\zeta_{\text{PPO}}$ varies by 3 orders of magnitude across the full composition range. In a PS/polycarbonate system, qualitatively similar effects are seen: the ratio of friction factors varies by a factor of 4, and each ζ displays a strong

* To whom correspondence should be addressed.

[†] Department of Chemistry, University of Minnesota.

[‡] Department of Chemical Engineering & Materials Science, University of Minnesota.

[§] Current address: Nanomaterials Research Corporation, Tucson AZ 85706.

maximum at intermediate compositions.⁴ In PS/poly-(vinylmethyl ether) ζ_{PS} increases by a factor of about 200 when $\phi_{PS} = 0.8$, compared to $\phi_{PS} = 1$ (again, the analysis is performed at constant $T - T_g$).⁵ One possible consequence of this phenomenon is the failure of time-temperature superposition in miscible blends, such as has been reported for poly(methyl methacrylate)/poly(ethylene oxide)⁶ and polyisoprene/poly(1,2-butadiene).^{7,8} However, this experimental approach is clearly not feasible for most polymer pairs, such as polystyrene/polyisoprene (PS/PI), where the two components are *immiscible*. In this paper we introduce a method utilizing ABAB tetrablock copolymers, whereby information about $\zeta_A(\phi, T)$ and $\zeta_B(\phi, T)$ may be obtained across the full composition range, even when A and B homopolymers are immiscible.

Multiblock copolymers in general offer interesting morphological and material properties, as well as thermodynamic features distinct from prototypical diblock copolymers. Here, however, we exploit a simple feature of multiblocks, namely that the order-disorder transition (ODT) temperature is considerably lower for an ABAB tetrablock than for the corresponding AB diblock with the same total M and composition, f . Specifically, we consider PS-PI tetrablocks with $M \approx 1.5 \times 10^4$ g/mol, and $f_{PS} = 0.23, 0.42, 0.60$, and 0.80 . The ODTs are all well below room temperature, whereas the corresponding symmetric diblock would have an ODT near 50°C . Consequently, each tetrablock provides a "homogeneous" matrix (on length scales greater than the chain dimensions) with a selected mixture of styrene and isoprene segments. Measurement of homopolymer tracer diffusion in such matrices would provide a direct route to $\zeta_A(\phi, T)$ and $\zeta_B(\phi, T)$. Tetrablock copolymers represent one step on the path between diblock and random copolymers, and random copolymers clearly represent a simple way to obtain homogeneous mixtures of normally immiscible components. However, the dynamic character of an A monomer can depend very much on the monomers to which it is bonded; the relaxation rate for styrene segments connected to isoprene segments is likely to differ substantially from the homopolymer case. The strategy, therefore, is to keep the block length sufficiently *short* that the ODT is suppressed, but sufficiently *long* that the (intramolecular) dynamic character of the constituents is retained.

The remainder of the paper is organized as follows. The synthesis and characterization of the tetrablock samples is described in the Experimental Section, as are the relevant experimental procedures: SANS, rheology, forced Rayleigh scattering (FRS), and pulsed-field gradient NMR. Then, SANS determination of the structure factor, $S(q)$, as a function of T is utilized to estimate the location of the ODT for each sample; the data are fit to a theoretical form for $S(q)$, based on the Leibler/RPA approach.⁹ The T dependence of the dynamic shear moduli, G' and G'' , and of η are reported for each tetrablock, and for PS and PI homopolymers of comparable total degrees of polymerization. Via time-temperature superposition, it is possible to estimate $\eta(f)$ at a fixed T ; because of the great difference in T_g between PS and PI, $\eta(f)$ spans approximately 20 orders of magnitude at room temperature and 3 orders of magnitude at 150°C . Glass transition temperatures are obtained from the T dependence of the low-frequency loss moduli. The self-diffusion coefficients of the tetrablocks and the homopolymers, obtained by NMR and

FRS, are then presented. In the Discussion, effective friction factors, $\zeta_{\text{eff}}(f, T)$ for the tetrablocks are extracted by treating each tetrablock as a pseudo-homopolymer that can be characterized by a single $\zeta(T)$; the friction factors determined from η and from D are shown to be consistent. We demonstrate that $\zeta_{\text{eff}}(f, T)$ cannot be predicted in any simple manner from the pure component values, $\zeta_{PS}^\circ(T)$ and $\zeta_{PI}^\circ(T)$. However, the dependence of ζ_{eff} on f at fixed $T - T_g$ is remarkably simple. This behavior identifies the composition dependence of T_g as the dominant influence on local friction in the mixture. Measurements of homopolymer tracer diffusion in the tetrablock matrixes are deferred to a future report.

Experimental Section

Samples. Four SISI tetrablock copolymers were prepared by sequential living anionic polymerization. Cyclohexane (Pure grade) was purchased from Phillips Petroleum, and *sec*-butyllithium and dibutylmagnesium were obtained from Lithium Corporation of America (Lithco) and used without further purification. Anionic polymerization grade isoprene was obtained from the Goodyear Corporation and used as received. Styrene was purchased from Aldrich and perdeuterostyrene (d_8) was purchased from Cambridge Isotopes. Both styrene and perdeuterostyrene were purified as needed by passing them through an activated alumina column to remove inhibitors, and then the monomers were added to a clean, dry round-bottom flask filled with nitrogen and fitted with rubber septa and a thermocouple. Dibutylmagnesium was added slowly until a persistent yellow/green color formed. This solution was then allowed to stir for a minimum of 1 h to react with trace impurities. The purified monomers were then isolated by distillation under vacuum from the mixture. To a clean reactor were added a fresh supply of cyclohexane and the desired amounts of purified styrene and perdeuterostyrene in a 3:1 mole ratio. The reactor was heated to 60°C and titrated by dropwise addition of *sec*-butyllithium. Once a persistent yellow color was achieved, the calculated amount of *sec*-butyllithium was charged to the reactor to give the desired molecular weight. A period of 30 min was allowed to permit complete conversion of the styrene, at which time a sample of the polystyrene first block was taken and then the desired amount of isoprene was added. After an additional 90 min to allow for complete conversion of the isoprene, a sample was taken and an additional quantity of purified styrene and per deuterostyrene monomers was charged to the reactor. After 30 min, a sample was taken and the final charge of isoprene was added. After 90 min had passed, the reaction was terminated with degassed 2-propanol. At 60°C these reaction times were more than sufficient to allow complete conversion. The contents of the reactor were pumped out under pressure and precipitated into a slightly acidic methanol/2-propanol mixture. The precipitated mixture was stabilized with Irganox 1010, vacuum-dried, and stored under refrigeration. Molecular weights and molecular weight distributions were determined by size exclusion chromatography with Ultrastaygel columns of 500, 1000, 10 000, and 100 000 Å porosities in tetrahydrofuran. Compositions were determined by ^1H NMR analysis using a GE QE-300 NMR. The resulting sample specifications are given in Table 1.

A PS homopolymer, $M_n = 1.3 \times 10^4$ and $M_w/M_n = 1.06$, was obtained from Pressure Chemical (Lot 30420) and a PI homopolymer, $M_n = 8.1 \times 10^3$ and $M_w/M_n \leq 1.1$, was generously provided by Dr. M. Hillmyer; these samples are designated PS-13 and PI-8, respectively. Portions of these polymers were labeled with the photochromic dye 4'-(*N,N*-dimethylamino)-2-nitrostilbene-4-carboxylic acid (ONS), to enable forced Rayleigh scattering measurements of chain diffusion. PS-13 was utilized in a previous study;¹⁰ the labels are distributed randomly along the chain, with an average of one label per eight chains. PI-8 was terminated with a hydroxyl group and was end-labeled by condensation with ONS in methylene

Table 1. Polymer Characteristics

sample	block molecular weight ^a				f^b	N^c
	styrene	isoprene	styrene	isoprene		
PI-8		8100			0.00	90
SISI-23	1400	4400	1600	4400	0.23	127
SISI-42	2600	3300	2900	3300	0.42	126
SISI-60	3000	1900	3500	1900	0.60	105
SISI-80	4900	1100	5200	1100	0.80	122
PS-13	13000				1.00	125

^a M_n , determined from stoichiometry, GPC, and NMR as described in the text. ^b Volume fraction of styrene, determined from stoichiometry and NMR, and using densities of 1.05 and 0.91 g/mL for PS and PI, respectively. ^c Total degree of polymerization referenced to the styrene monomer volume.

chloride, using 1,3-dicyclohexylcarbodiimide and 4-(dimethylamino)pyridine as catalysts.

Small-Angle Neutron Scattering. SANS measurements were performed at the National Institute of Standards and Technology (NIST) on the 30 m Exxon/University of Minnesota/NIST (NG7) instrument. The incident wavelength, λ , was 7 Å with a dispersion, $\Delta\lambda/\lambda$, of 0.10. The sample-to-detector distance was 1.25 m, the source aperture was 5.0 cm, the sample aperture was 0.95 cm, and the detector was offset by 25 cm to provide a usable q range of 0.03 to 0.4 Å⁻¹, where q is the usual scattering vector ($= (4\pi/\lambda) \sin(\theta/2)$). Samples were contained between quartz disks, using an aluminum spacer ring and a high-temperature adhesive. Temperature was controlled to within ± 0.5 °C using resistive heaters and monitored via a calibrated thermocouple embedded in a blank cell containing water. Measurements were also performed on PS and PI homopolymers to provide an estimate of the incoherent contribution to the signal from each tetrablock.

The data were corrected for transmission, sample thickness, background, detector sensitivity, and window contributions and then placed on an absolute scale using a calibrated water standard. The azimuthally averaged data, $I(q)$, were then corrected for the incoherent scattering to extract the coherent contribution, $I_{\text{coh}}(q)$ (or $d\Sigma/d\Omega$) in units of cm⁻¹. The structure factor peaks were sufficiently broad that smearing corrections were unnecessary.

Rheology. Measurements were made on Rheometrics RSA-II, RMS-800, or DSR rheometers, as appropriate. Sample chamber temperatures were controlled to within ± 1 °C with a steady flow of nitrogen that also inhibited sample degradation. In all cases strain sweeps were performed to establish that the measurements were taken in the linear viscoelastic regime. Temperature sweeps were performed on all six samples to determine an effective glass transition temperature, taken as the temperature at which G'' exhibits a maximum (at 1 rad/s).

Forced Rayleigh Scattering. FRS measurements were made on the instrument described previously, in the amplitude grating mode.¹¹ The homopolymer samples contained 6.2% (PI) or 3.8% (PS) of the labeled species. Temperatures were controlled to within ± 0.2 °C using resistive heaters and a calibrated RTD. Each FRS decay was fit to a single exponential function to extract the decay rate, as previously described.¹⁰ For each sample, the grating spacing was varied to confirm that the decay rate varied linearly with the square of the grating wavevector, as required for a diffusive process.

Pulsed-Gradient Spin-Echo NMR. Center-of-mass diffusion measurements were performed using the large-pulsed-gradient spin-echo NMR method pioneered by Stejskal and Tanner;¹² our implementation has been described in detail elsewhere.¹³ Nonspectroscopic pulsed ¹H NMR was performed at 33 MHz in a conventional electromagnet using several home-built variable-temperature field-gradient probes, either on-resonance or in single-sideband FT mode. The attenuation of the principal or stimulated spin-echo was measured as a function of the duration δ of the field gradient pulses. Gradient strengths between $G = 130$ and 524 G/cm were used; a steady gradient of 0.8 G/cm was also applied. At high G and

larger δ we employed δ -dependent differential gradient pulse length corrections, and compensated for receiver phase shifts. Where required, the data reduction program¹⁴ corrected for small residual gradient effects.¹⁵

Principal echo spin-spin relaxation (T_2) measurements were also performed on several specimens. Two-component decays were generally observed, with the longer exponential component (relied on by the diffusion measurements, particularly at lower temperatures) arising from the isoprene blocks. The polymer molecular weight dispersity in this work was too small to benefit from fitting an explicit simulation of its diffusivity distribution. The model¹⁴ fitted to the spin-echo data usually employed a single diffusion coefficient, except at the lowest temperatures, where even T_2 of the isoprene blocks was short enough for trace volatile contaminants with long T_2 to become apparent; in this situation a small, rapid component was included in the fit.

Results

Structure Factor. The structure factor for a regular ABAB tetrablock copolymer in the disordered state may be calculated following the mean-field approach of Leibler,⁹ utilizing the random phase approximation (RPA); "regular" is used to indicate that for each component the two blocks have the same degree of polymerization. The general result may be expressed as^{9,16}

$$S(q) = \frac{N}{F(x) - 2\chi N} \quad (1)$$

where $F(f, x)$ represents an appropriate combination of Debye functions $g(f)$

$$g(f) \equiv \frac{2}{x^2} \{e^{-fx} + fx - 1\} \quad (2)$$

with $x = q^2 R_g^2$. For the regular tetrablock, the first A block runs from 0 to $fN/2$, the first B block from $fN/2$ to $N/2$, and the second A block from $N/2$ to $(1 + f)N/2$. The result is

$$F(f, x) = \frac{N\{S_{11} + 2S_{12} + S_{22}\}}{\{S_{11}S_{22} - S_{12}^2\}} \quad (3)$$

where the partial structure factors S_{ij} are given by

$$\frac{S_{11}}{N} = 2g\left(\frac{f}{2}\right) + g\left(\frac{1-f}{2}\right) + g\left(\frac{1+f}{2}\right) - 2g\left(\frac{1}{2}\right) \quad (4a)$$

$$\frac{S_{22}}{N} = 2g\left(\frac{1-f}{2}\right) + g\left(\frac{f}{2}\right) + g\left(\frac{2-f}{2}\right) - 2g\left(\frac{1}{2}\right) \quad (4b)$$

$$\frac{S_{12}}{N} = \frac{1}{2} \left\{ 4g\left(\frac{1}{2}\right) + g(1) - 3g\left(\frac{1-f}{2}\right) - 3g\left(\frac{f}{2}\right) - g\left(\frac{2-f}{2}\right) - g\left(\frac{1+f}{2}\right) \right\} \quad (4c)$$

As expected for any disordered, monodisperse block copolymer, $S(q)$ vanishes as $q \rightarrow 0$, and exhibits a peak at a finite q^* . The peak intensity diverges at the spinodal, χ_s , which we will take as a reasonable estimate of the ODT.

The experimental $S(q)$ values are shown in Figure 1A–D, for SISI-23, -42, -60, and -80, respectively. The accessible temperature range decreases with increasing styrene content, due to the higher T_g and the concomitant loss of equilibrium upon cooling. The fits to eq 1

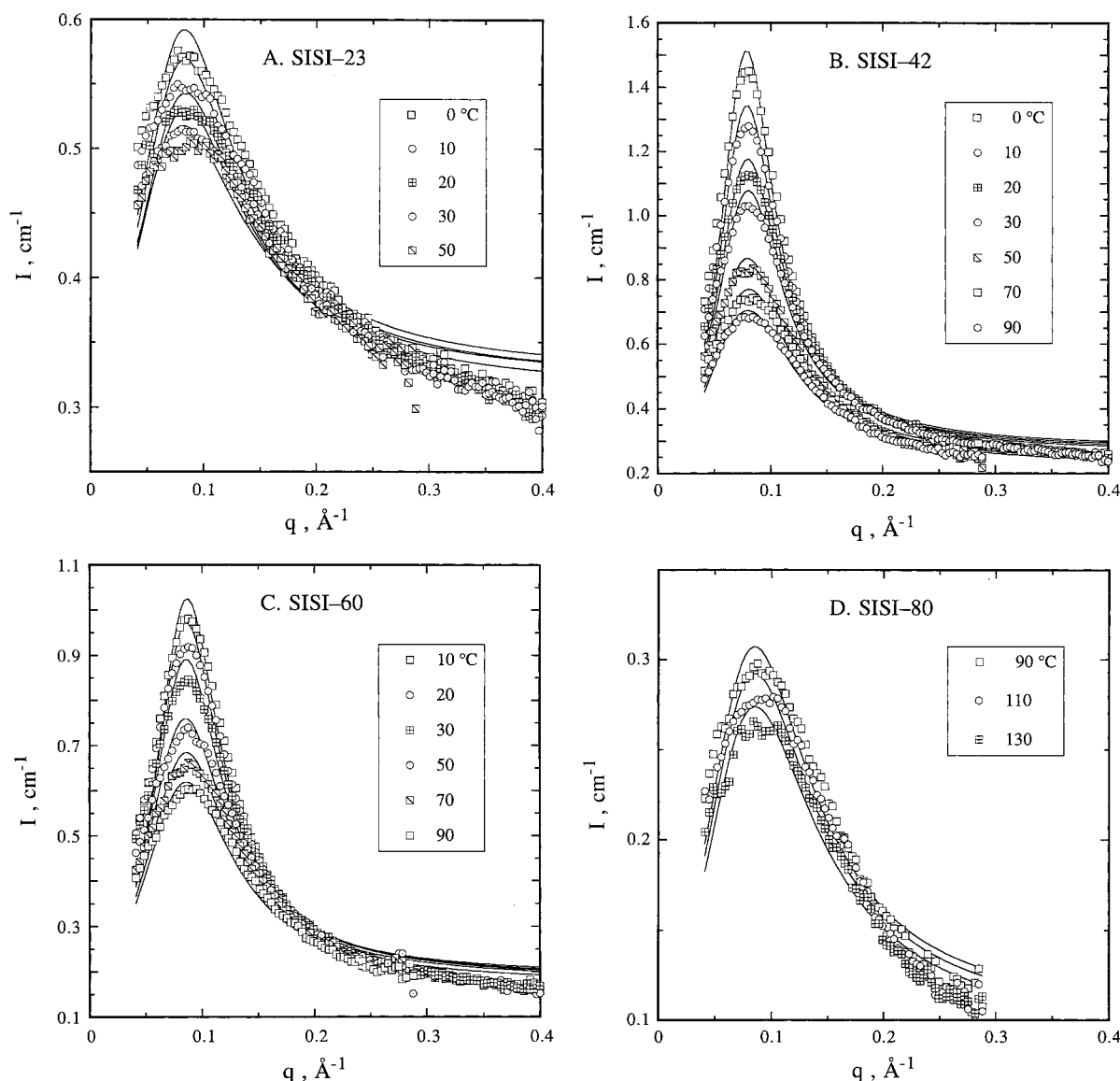


Figure 1. SANS scattering curves as a function of temperature, and the associated Leibler/RPA structure factor fits, for (A) SISI-23, (B) SISI-42, (C) SISI-60, and (D) SISI-80.

are generally reasonable, but the experimental peaks are systematically broader (an effect which is attributable to dispersity in both N and, especially, f). Three parameters are extracted from each fit: R_g , χ , and a residual baseline term. In all cases, R_g is independent of T , and equal to 40.7 , 39.4 , 36.5 , and 40.1 ± 0.5 Å, for SISI-23, -42, -60, and -80, respectively. These results are systematically larger than the values one would obtain using the statistical segment lengths of PS (6.7 Å) and PI (6.5 Å) and the values of N in Table 1; they imply an effective statistical segment length of ca. 8.8 Å. This apparent discrepancy is consistent with results on diblock copolymers, both in sign and magnitude, where chain stretching has been implicated.¹⁷ The T independence of R_g , which is inferred from the T independence of q^* , is in agreement with mean-field theory but differs from the experimental results on diblock copolymers.¹⁸ This reflects both the large distance to the ODT and the more mean-field character of the tetrablock architecture. The values of χ fall in the range 0.1 to 0.3 , consistent with other results in the literature,¹⁹ and have the expected linear dependence on T^{-1} . However, the absolute values are rather sensi-

tive to the issue of polydispersity, so we do not emphasize them here.

The mean-field ODTs may be estimated by extrapolation of $I^{-1}(q^*)$ vs T^{-1} , as shown in Figure 2; for this purpose $I(q^*)$ is obtained by fitting the peak to a Gaussian function. The resulting estimates are -130 , -50 , -60 , and -70 °C, for the four copolymers in order of increasing styrene content. These values are all substantially below room temperature, and thus well outside the T range of interest for $\zeta(T)$, which we take to be 25 – 180 °C. Interestingly, these extrapolations are all quite linear; there is no evidence of a fluctuation regime as the ODT is approached. Since the extrapolation range is quite large, the significance of this observation is limited. However, if fluctuations do grow in at lower temperatures, they should only suppress the ODT further, and so our principal conclusion is robust: on length scales greater than the chain dimensions, the tetrablock copolymers represent homogeneous matrices of styrene and isoprene segments.

Rheology. The viscoelastic properties of the four tetrablocks and the two homopolymers are shown in Figure 3, as a function of reduced frequency ωa_T . The

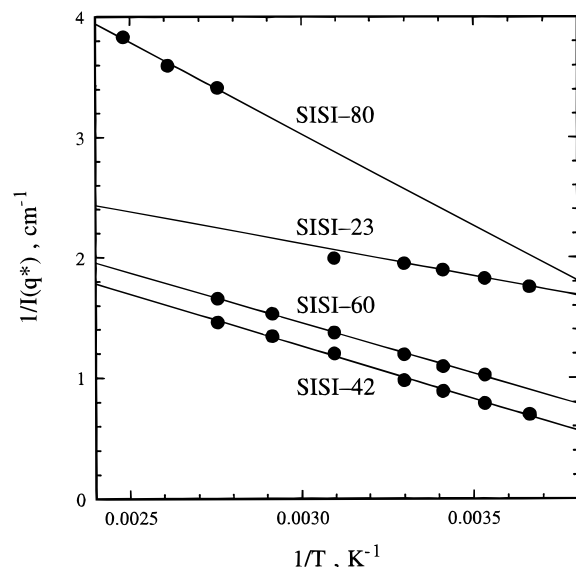


Figure 2. Inverse peak intensity vs inverse temperature, and the associated linear regression fits used to obtain estimates of the mean-field ODT.

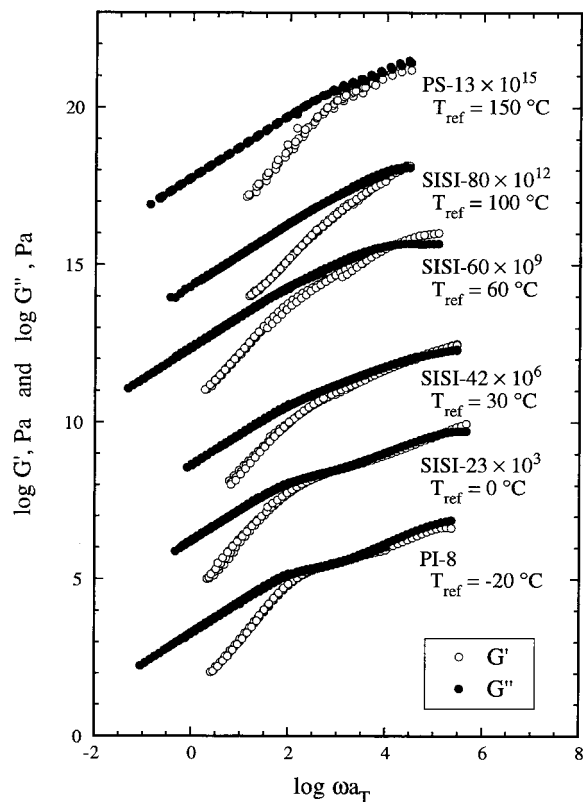


Figure 3. Dynamic shear moduli as a function of reduced frequency. Reference temperatures and vertical displacements were identified on plot.

reference temperature is different for each material in order to bring the longest relaxation times into the same reduced frequency window, and the various moduli have been multiplied by the indicated factors to provide vertical separation. For each sample the data represent master curves obtained from the superposition of data obtained at several (from five to nine) different temperatures. Generally the superposition is excellent; the empirical time-temperature superposition shift factors, a_T , follow the WLF equation (eq 5). There is some suggestion of a breakdown in superposition for SISI-

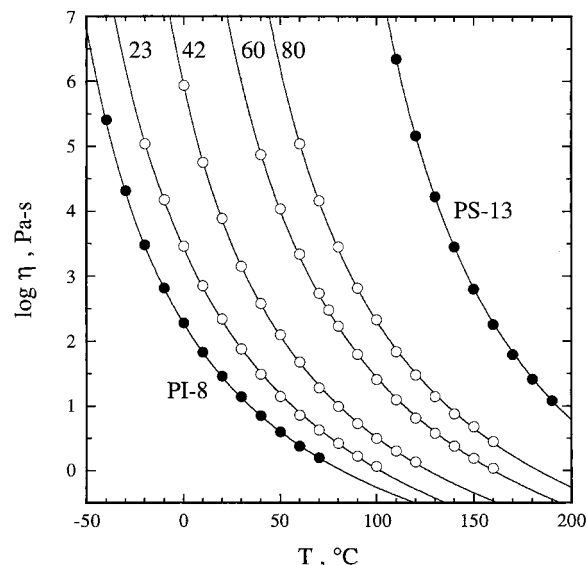


Figure 4. Zero-shear-rate viscosity as a function of temperature. Smooth curves represent fits to the WLF equation.

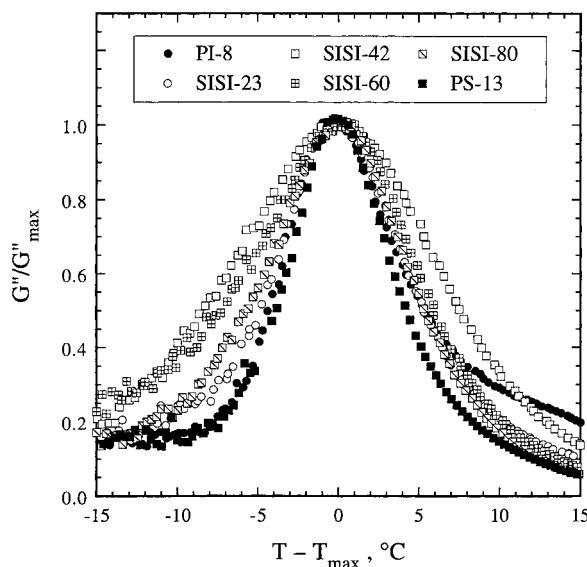


Figure 5. Normalized loss modulus as a function of temperature, relative to the temperature of the maximum in G'' .

60, which may be correlated with the dispersion of the G' peak to be discussed subsequently (see Figure 5). The data fall predominantly in the terminal regime, and thus enable determination of $\eta(T)$. With increasing isoprene content, the G' and G'' curves begin to overlap at a frequency closer to the inverse longest relaxation time, which is a first signature of the onset of entanglement coupling.² Nevertheless, it is clear that all six samples may be considered to be unentangled.

The temperature dependence of the zero shear rate viscosity for the six samples is shown in Figure 4. For a given sample, $\eta(T)$ ranges over as many as 6 orders of magnitude, and a smooth progression with increasing styrene content is evident. In each case the data are well described by the WLF function

$$\log\left(\frac{\eta(T)}{\eta(T_{\text{ref}})}\right) = \log a_T = \frac{-C_1(T - T_{\text{ref}})}{C_2 + (T - T_{\text{ref}})} \quad (5)$$

where the parameters C_1 and C_2 depend on the choice

Table 2. WLF Parameters Based on the Temperature Dependence of Viscosity

sample	C_1	$C_2, ^\circ\text{C}$	$T_{\text{ref}}, ^\circ\text{C}$
PI-8	6.530	88.5	-20
SISI-23	7.305	111.8	0
SISI-42	6.895	110.6	30
SISI-60	7.160	112.5	60
SISI-80	5.404	114.7	100
PS-13	6.817	116.9	150

of reference temperature. These values are given in Table 2, with the reference temperatures identical to those in Figure 3.

To obtain a consistent estimate of the glass transition temperature for the six samples, the dynamic shear moduli were measured as a function of increasing temperature (1 $^\circ\text{C}/\text{min}$) at a fixed frequency (1 rad/s) and low strain amplitude (1%). For high molecular weight polymers, a distinct peak in $\tan \delta$ would be observed, corresponding to the transition zone of viscoelastic behavior. For these low molecular weight materials there is no clear separation of the transition and terminal regimes, and $\tan \delta$ is not so informative. However, in all cases a distinct maximum in the loss modulus, G'' , is observed, at $T = -54.3, -44.3, -15.6, +20.9, +39.4$, and $+104.5$ $^\circ\text{C}$, respectively, for the samples in order of increasing styrene content. For the two homopolymers these temperatures are approximately 10 $^\circ\text{C}$ above the T_g values obtained by DSC, which can be attributed to the finite frequency in the rheological measurements; clear calorimetric transitions were not consistently observed for the tetrablocks. The values of G'' in the vicinity of the maximum are plotted in reduced format (G''/G''_{max} vs $T - T_{\text{max}}$) in Figure 5. One interesting feature that emerges from this comparison is that the tetrablocks exhibit broader dispersions than the homopolymers; the effect is largest for the midcomposition samples SISI-42 and -60. This implies an underlying dynamic heterogeneity, or a broader distribution of segmental relaxation times, for these materials. A fuller investigation of the significance of this observation will require measurements of the individual segmental relaxation times, for example by dielectric relaxation, depolarized light scattering, or NMR. Perhaps more importantly, however, the fact that all four tetrablocks exhibit a single peak in $G''(T)$ places a limit on the possible difference in effective T_g s that the styrene and isoprene segments sense in a given matrix. The T_g s thus determined are plotted in Figure 6, as a function of styrene weight fraction, w_{PS} . They are compared with the prediction of the Fox equation

$$\frac{1}{T_g} = \frac{w_{\text{PS}}}{T_{g,\text{PS}}} + \frac{w_{\text{PI}}}{T_{g,\text{PI}}} \quad (6)$$

which is often applied successfully to random copolymers.²⁰ The agreement is by no means perfect, as the data show a stronger dependence on composition at the high PS end, but a weaker dependence at the low PS end. This is presumably attributable to the blockiness of the polymers. Comparison with other expressions for the composition dependence of T_g , such as the Gordon-Taylor²¹ and Couchman²² equations, give very similar results when literature values for the relevant parameters are employed.

Diffusion. The combined FRS and NMR measurements of self-diffusion for the six samples are shown in Figure 7, as a function of temperature. The NMR

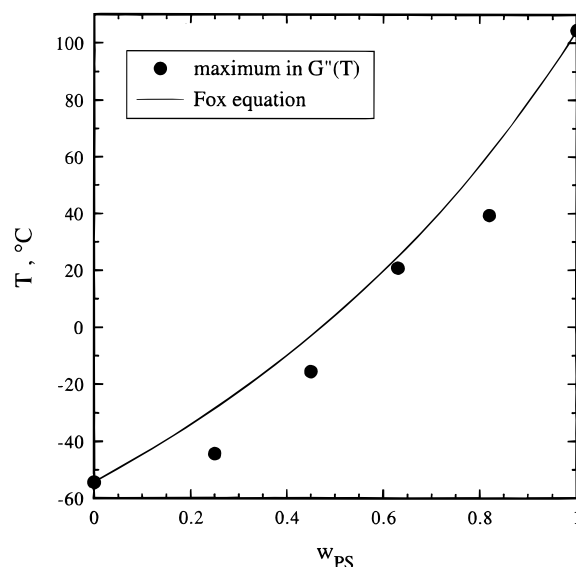


Figure 6. Glass transition temperatures, taken as the temperature of the maximum in $G''(T)$, vs styrene weight fraction. The prediction of the Fox equation is also shown.

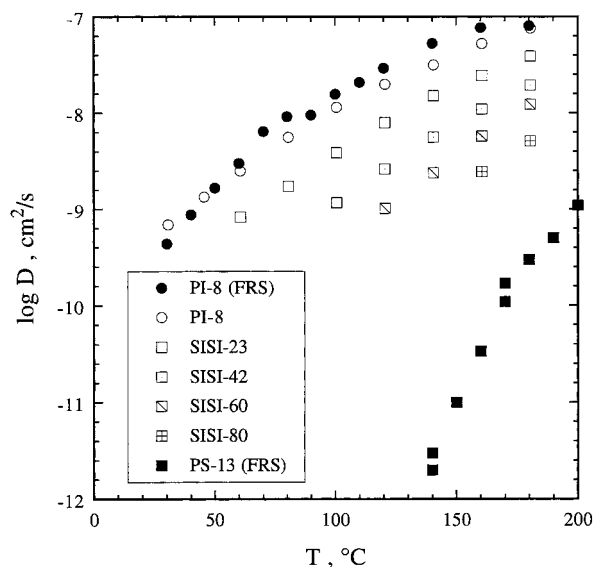


Figure 7. Self-diffusion coefficients by NMR and FRS as a function of temperature.

experiment has the virtue of requiring no chemical modification to the samples, but it has a restricted dynamic range relative to FRS. Consequently, the number of NMR data points decreases with increasing styrene content. However, for PI-8 extensive measurements were possible with both techniques, and the results compare favorably. The FRS measurements on PS-13 were reported previously.¹⁰ Overall the data are as expected: D increases with isoprene content at fixed T , and the T dependence becomes stronger with increasing styrene content, due to the proximity of T_g .

Discussion

To couch the ensuing discussion in terms of ζ , it is necessary to extract ζ from the measured $\eta(T)$ and $D(T)$ via a model. For this we employ the Rouse theory expressions, applicable to unentangled molten polymers²

$$D = \frac{kT}{N\zeta} \quad (7)$$

$$\eta = \frac{\rho N_{av}}{36M_0} N b^2 \zeta \quad (8)$$

where N is the degree of polymerization, N_{av} is Avogadro's number, M_0 is the monomer molecular weight, ρ is the density, and b is the statistical segment length. For the tetrablocks, we extract an effective friction factor, ζ_{eff} , by assuming the homopolymer formulas above, and using appropriate averages for ρ and M_0 . The statistical segment lengths for PS and PI are taken as 6.7 and 6.5 Å, respectively, and Gaussian statistics are assumed. We thus employ calculated radii of gyration, rather than those inferred from the structure factor fits, as the latter are model-dependent.

The strict applicability of the Rouse expressions may be questionable for at least two reasons. First, the linear scaling of $1/D$ or η with M is generally seen only after correction for chain end effects are made, due primarily to the M dependence of T_g . Clearly, we do not have a series of tetrablock samples with varying N but constant composition to test this proposition. However, as the value of N is reasonably constant for all six samples considered (see Table 1), the values of ζ_{eff} should at least be internally consistent. Second, the PI homopolymer has $M_e < M < M_c$, and thus the possibility exists that incipient entanglements influence the dynamics slightly. It is clear, however, that none of these polymers is well-entangled, and thus the reptation model is not applicable; consequently, we can neglect this small possible contribution.

The combined diffusion- and viscosity-based ζ_{eff} are shown as a function of T in Figure 8. The agreement between diffusion and viscosity is gratifying, although not unexpected, as both quantities are determined primarily by the longest relaxation time of the chain. There appears to be a slight discrepancy for SISI-42, with the diffusion-based friction factor being larger. This might be correlated with the width of the $G''(T)$ peak evident in Figure 5. Also shown are WLF fits to the combined data sets; the resulting parameters are given in Table 3, in this case utilizing the glass transition temperatures in Figure 6 as the reference temperatures. Clearly ζ_{eff} is a strong function of composition at fixed T . Note, however, that ζ_{eff} changes much more between SISI-80 and pure PS, than between pure PI and SISI-23. In some sense, this implies that isoprene is much more effective at plasticizing styrene than styrene is in retarding the segmental motion of isoprene. This inference was also drawn from the T dependence of the self-diffusion of a styrene–isoprene diblock copolymer²³ and can be understood qualitatively in the following manner. Segmental dynamics generally reflect a combination of intra- and intermolecular constraints, with the relative proportion dependent on monomer structure, temperature, and composition. In the limit where intermolecular interactions completely dominate one might anticipate that the segmental dynamics of both components would exhibit a similar T dependence, as their motions would be completely coupled. On the other hand, if only intramolecular constraints contribute, one might observe two different T dependences in a homogeneous mixture, leading, for example, to the failure of time–temperature superposition.^{6,7} In this particular mixture, styrene apparently is more sensitive

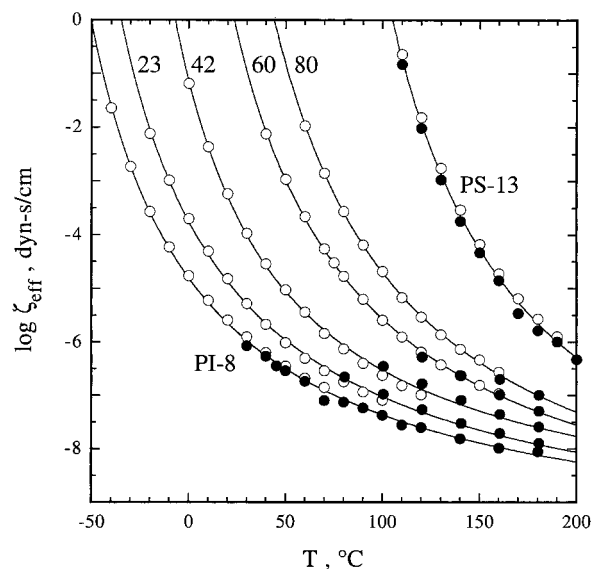


Figure 8. Effective monomeric friction factors, as defined in the text, from viscosity (open symbols) and self-diffusion (filled symbols) measurements, as a function of temperature. Smooth curves represent fits to the WLF equation.

Table 3. WLF Parameters Based on the Temperature Dependence of the Effective Friction Factors

sample	$C_1 g$	$C_2 g, ^\circ\text{C}$	$T_g, ^\circ\text{C}$	$\log [\zeta_{eff}(T_g)]^a$
PI-8	10.8	51.1	−54.3	0.75
SISI-23	12.0	49.3	−44.3	1.91
SISI-42	11.6	44.6	−15.6	1.87
SISI-60	10.8	64.6	20.9	0.37
SISI-80	11.4	65.3	39.4	0.77
PS-13	11.0	69.8	104.5	0.08

^a Friction factors in units of (dyn s)/cm.

to intermolecular constraints than isoprene. This is consistent with the results of Gisser and Ediger, who found that whereas local motions of PS in solution exhibited relaxation times that scaled approximately with the solvent viscosity, those of PI depended much less strongly on the viscosity of the medium.²⁴ A simplistic interpretation of this phenomenon relies on segment size. In PS, backbone rearrangements require motion of the relatively large phenyl rings through the medium, whereas PI conformational changes implicate only one methyl substituent every four backbone atoms.

It is instructive to examine the composition dependence of ζ_{eff} at fixed $T - T_g$, as in the work on miscible blends.^{3,5} It is sometimes inferred that this is approximately an iso-free volume state, although calculations to be presented in the Appendix indicate that this is far from the case for PS/PI mixtures. The results are shown in Figure 9A, for three different values of $T - T_g$. Rather remarkably, perhaps, under these conditions ζ_{eff} is only a weak function of composition. This should be contrasted with the PS/PPO and PS/PVME blends, where ζ_{PS} varied by 2 orders of magnitude or more with composition under equivalent conditions.^{3,5} However, it is important to recall that ζ_{eff} averages over both ζ_{PS} and ζ_{PI} , and conceivably either of these quantities could have a much stronger f dependence. This will be the subject of a subsequent report, but preliminary measurements of homopolymer diffusion in the tetrablocks indicate that the component friction factors are not greatly different from ζ_{eff} . In Figure 9B we show the six friction factors from Figure 8 plotted directly as a function of $T - T_g$; consistent with the data in Figure

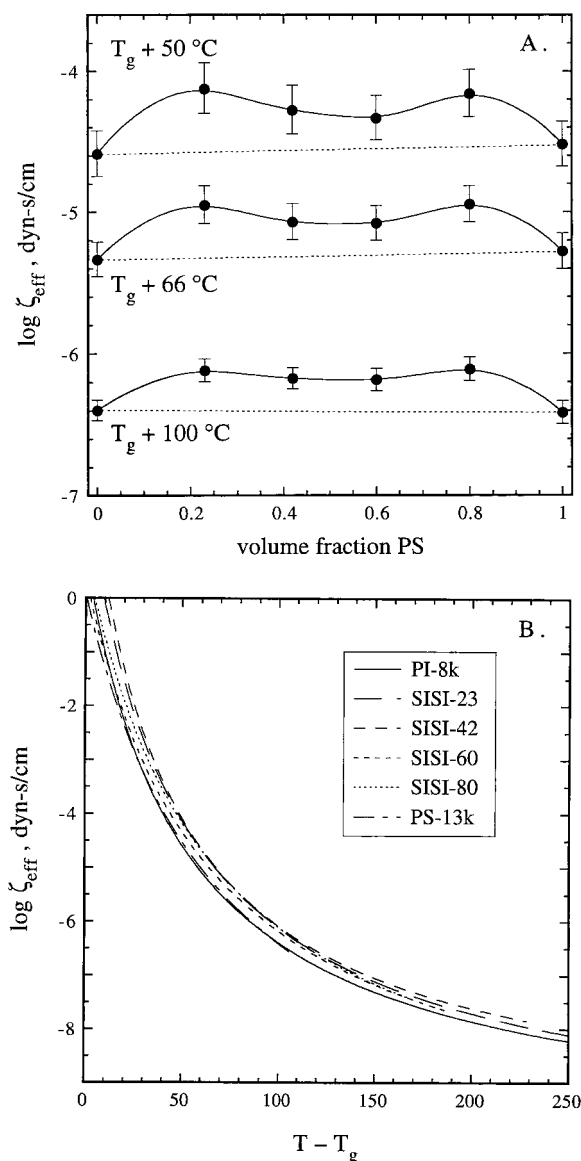


Figure 9. Effective monomeric friction factors as (A) a function of composition, at fixed distances above the sample T_g , and (B) as a function of $T - T_g$. The error bars in part A represent the effect of $\pm 3^\circ\text{C}$ uncertainty in the assignment of T_g (see Figure 6).

9A, this simple reduction captures almost all of the f dependence, and highlights the similar T dependences. The similarity in the curves in Figure 9B underscores that the variations among the WLF parameter values listed in Table 3 are not particularly significant.

Close inspection of Figure 9 reveals that the tetrablocks have systematically slightly higher friction factors than the homopolymers, particularly for the less symmetric compositions. This may be interpreted in several ways. One simple explanation is that one component, e.g., styrene, dominates the response, and thus the f dependence of ζ_{eff} is essentially the f dependence of ζ_{PS} . However, the preliminary measurements of $\zeta_{\text{PS}}(f)$ suggest that this is not the case. Another possibility is a *thermodynamic* contribution to ζ_{eff} , in the sense that there is a very weak association between like blocks on different chains. Such an association is obviously not too strong, given the success of the mean-field prediction for the structure factor. However, if one posits that chain mobility is then inhibited by a thermodynamic barrier, the barrier would presumably scale

as $f(1 - f)\chi N$

$$\eta^{-1} \sim D = D_0 \exp[-\alpha f(1 - f)\chi N] \quad (9)$$

where D_0 is the diffusivity in the absence of associations (at fixed $T - T_g$) and α is an unknown constant.

We now consider possible ways to predict $\zeta_{\text{eff}}(f, T)$ from the homopolymer values $\zeta_{\text{PS}}^\circ(T)$ and $\zeta_{\text{PI}}^\circ(T)$. Although there is no a priori reason to expect that this can be done successfully for any system, the rather smooth and monotonic dependence of ζ_{eff} on temperature and composition in PS/PI provides some basis for optimism. The approach we adopt is to employ a series of mixing rules that differ in how they envision the changes in molecular environment to influence segmental mobility. We first adopt a mixing rule for ζ_{eff} in terms of ζ_{PS}° and ζ_{PI}° , and then select the appropriate values of ζ_{PS}° and ζ_{PI}° to utilize for a given temperature and composition.

For the mathematical form of the mixing rule, two candidates are considered: the volume fraction-weighted arithmetic average

$$\zeta_{\text{eff}} = f_A \zeta_A^\circ + f_B \zeta_B^\circ \quad (10)$$

and the volume fraction-weighted geometric mean

$$\zeta_{\text{eff}} = (\zeta_A^\circ)^{f_A} (\zeta_B^\circ)^{f_B} \quad (11)$$

Equation 10 amounts to assuming that the total friction felt by a chain is the sum of the friction felt by each monomer and is thus similar in spirit to the Rouse model. Equation 11 falls in the class of Friedman–Porter mixing rules commonly employed to describe the effects of blending on polymer physical properties²⁵ and is analogous to an often-successful empirical relationship for the viscosity of mixtures of small molecules,²⁶ originally proposed by Arrhenius.²⁷ Due to the enormous difference between ζ_{PS}° and ζ_{PI}° , only the PS contribution to ζ_{eff} is significant in eq 10, and the resulting predictions are invariably far from experiment. Consequently, we restrict ourselves to eq 11 and consider four different methods for selecting the input to eq 11.

Method 1. The friction experienced by a monomer in the mixture is taken to be equivalent to that for a homopolymer at the same temperature; i.e., no adjustment is made for the change in local environment upon mixing, except for that embodied in eq 11. Since the average molecular weight for each tetrablock is small, the ζ° inputs at a given temperature depend strongly on the choice of homopolymer molecular weight, due to the well-known M dependence of T_g at small M . Homopolymers of the same molecular weight as the tetrablocks are used in this first proposal. The WLF fits to the data for PS-13 and PI-8, which closely satisfy the condition of equivalent M , are thus employed.

Method 2. A monomer is again assumed to experience the same friction in the mixture as it does in the homopolymer at a given temperature. However, to address the possibility that monomer dynamics are more sensitive to constraints imposed at the block level than by the entire chain, it is further assumed that each component retains the dynamic character of a homopolymer with a chain length equal to the respective block length, without regard to block connectivity. The $\zeta^\circ(T)$ values for such low molecular weight homopolymers are approximated by shifting the measured ζ_{PS}°

Table 4. Temperature Shifts Used in "Method 2" (See Text) To Account for the Reduced T_g of a Homopolymer of Block Molecular Weight M (Number Average), Relative to PS-13 ($M_n = 13\,000$) or PI-8 ($M_n = 8100$)

tetrablock	M (PS block)	$\Delta T_g^{\text{PS}}, ^\circ\text{C}$	M (PI block)	$\Delta T_g^{\text{PI}}, ^\circ\text{C}$
SISI-23	1500	-52.0	4400	-1.8
SISI-42	2750	-29.3	3300	-3.1
SISI-60	3250	-24.5	1900	-7.1
SISI-80	5050	-14.2	1100	-13.8

(T) and $\zeta_{\text{PI}}^\circ(T)$ curves along the temperature axis by a factor $\Delta T_g = T_g(\text{block } M) - T_g(\text{homopolymer } M)$, where $T_g(M)$ is calculated using relationships from the literature

$$T_g(M) \text{ in } ^\circ\text{C} = -68.8 - 17600M^{-1} \quad (12a)$$

for PI,²⁸ and

$$T_g(M) \text{ in } ^\circ\text{C} = 105 - 8935M^{-2/3} \quad (12b)$$

for PS,²⁹ with M being the number-average molecular weight. The resulting shift factors are presented in Table 4. In practice, the new $\zeta_{\text{PS}}^\circ(T)$ and $\zeta_{\text{PI}}^\circ(T)$ inputs are generated by substituting ($T_g + \Delta T_g$) for the reference temperature in the WLF equation for each homopolymer, using the values for C_1^g , C_2^g , and $\log \zeta_{\text{eff}}(T_g)$ given in Table 3.

Method 3. The PS and PI blocks in the mixture are still assumed to retain the dynamic character of the corresponding homopolymers at the same temperature, but now the "plasticization" effects associated with mixing two components with different dynamic properties are taken into consideration. That is, the effective T_g and friction factor for PS monomers are expected to decrease upon mixing, whereas those for PI monomers are expected to increase. Since we cannot predict the extent of these effects a priori, we assume a common effective glass transition, $T_g^{\text{eff}}(f)$, for both components. Values for $T_g^{\text{eff}}(f)$ are calculated using the Fox equation, rather than using those from $G'(T)$, so as to follow the principle of using only homopolymer properties in the mixing rule. $\zeta^\circ(T)$ values corresponding to these states of plasticization are approximated by shifting the measured $\zeta_{\text{PS}}^\circ(T)$ and $\zeta_{\text{PI}}^\circ(T)$ curves along the temperature axis by $\Delta T_g = T_g^{\text{eff}}(\text{tetrablock}) - T_g^{\text{eff}}(\text{homopolymer})$. The qualitative success of this reduction in Figure 9B anticipates the success of this approach.

Method 4. On the basis of the assumption that segmental mobility depends primarily on restrictions imposed by the packing of segments in the local environment, the friction experienced by a monomer in the mixture should be same as that in the homopolymer under conditions which yield an equivalent local density; the effect of temperature enters indirectly through this relationship. This proposal can be quantified using the well-established concept of free volume. For example, ζ is often assumed to exhibit an exponential dependence on fractional free volume, $f_{\text{FV}} = V_{\text{free}}/V$ where V_{free} is the free volume and V is the total volume:^{2,30}

$$\zeta \sim \exp(\gamma V^*/f_{\text{FV}}) \quad (13)$$

V^* is a measure of the occupied volume, and the parameter γ varies with molecular structure and interactions with the local environment. Employing a simple definition of free volume, $V_{\text{free}} = V - V^*$, the fractional free volume is given by $f_{\text{FV}} = 1 - V^*/V$. In the Appendix,

we use the Sanchez–Lacombe equation of state^{31,32} to calculate f_{FV} for the homopolymers and tetrablocks on this basis. The resulting parametrization of $f_{\text{FV}}(f, T)$ allows us to calculate the temperatures T_{PS} and T_{PI} necessary to achieve the same fractional free volume as found in a tetrablock at temperature T (see Figure 11 in the Appendix). We then use $\zeta_{\text{PS}}^\circ(T_{\text{PS}})$ and $\zeta_{\text{PI}}^\circ(T_{\text{PI}})$ to predict $\zeta_{\text{eff}}(T)$. To avoid confusing the effects of this "constant free volume" assumption with the homopolymer molecular weight dependence discussed in methods 1 and 2, the ζ° values employed are for high molecular weight PS and PI. Consequently, the measured curves for PS-13 and PI-8 are shifted along the temperature axis to produce the new $\zeta_{\text{PS}}^\circ(T)$ and $\zeta_{\text{PI}}^\circ(T)$ curves; in this case, $\Delta T_g^{\text{PS}} = 16.2 ^\circ\text{C}$ and $\Delta T_g^{\text{PI}} = 2.2 ^\circ\text{C}$.

Predictions based on these four methods are presented in parts A–D of Figure 10 as solid curves 1–4, respectively. Clearly, none of the methods describe the data quantitatively, with the PS contribution to $\zeta_{\text{eff}}(f, T)$ overestimated in each case. Treatment of the PS glass transition plays a critical role in this respect, since methods 1–3, which involve progressively lower estimates of $T_g(\text{PS})$, yield progressively better agreement with the data. Such improvement is due in large part to the fact that $T_g(\text{PS})$ sets the temperature at which $\zeta_{\text{eff}}(f, T)$ is predicted to diverge. The prediction from Method 3, which assumes a common T_g^{eff} for both components somewhat above the measured T_g , is actually quite good, particularly with regard to the temperature dependence. If this method were applied using the measured T_g values instead, the curves would fall slightly too far to the PI side of the data; thus, an optimal value between $T_g(\text{measured})$ and T_g^{eff} (Fox equation) would produce a nearly quantitative fit. Consequently, the task of predicting $\zeta_{\text{eff}}(f, T)$ for PS/PI reduces to the problem of predicting $T_g^{\text{eff}}(f)$, as also implied by Figure 9B.

It is also apparent from the results in Figure 10 that the free volume approach, although yielding a poor quantitative description, does capture the effect of mixing qualitatively. Furthermore, if we employ homopolymer curves that account for the decrease in T_g experienced by a monomer in the mixture relative to the pure state, the agreement is dramatically improved. For example, using the approach outlined in method 2 in which $T_g(\text{PS})$ and $T_g(\text{PI})$ are estimated from the block molecular weights without considering plasticization effects, the predictions based on constant f_{FV} mixing are quantitatively similar to method 3. However, meaningful further development of this approach can only occur after we obtain a better understanding of the T_g "sensed" by each monomer in the mixture.

The general failure of the mixing rules in Figure 10 reinforces the idea that the PI contribution to $\zeta_{\text{eff}}(f, T)$ is more significant than expected based on composition alone. This behavior mimics the composition dependence of T_g in Figure 6, where a large depression is observed with the addition of PI to pure PS, and only a slight increase occurs upon addition of PS to pure PI. In terms of the discussion of Figure 8, ζ_{PS} is more affected by intermolecular constraints than is ζ_{PI} , possibly due to the larger side-group structure. The mixing rules only capture this asymmetry when they incorporate a strong composition dependence of $T_g(\text{PS})$; otherwise, the PS component is treated as if it were in the glassy state over too much of the temperature range.

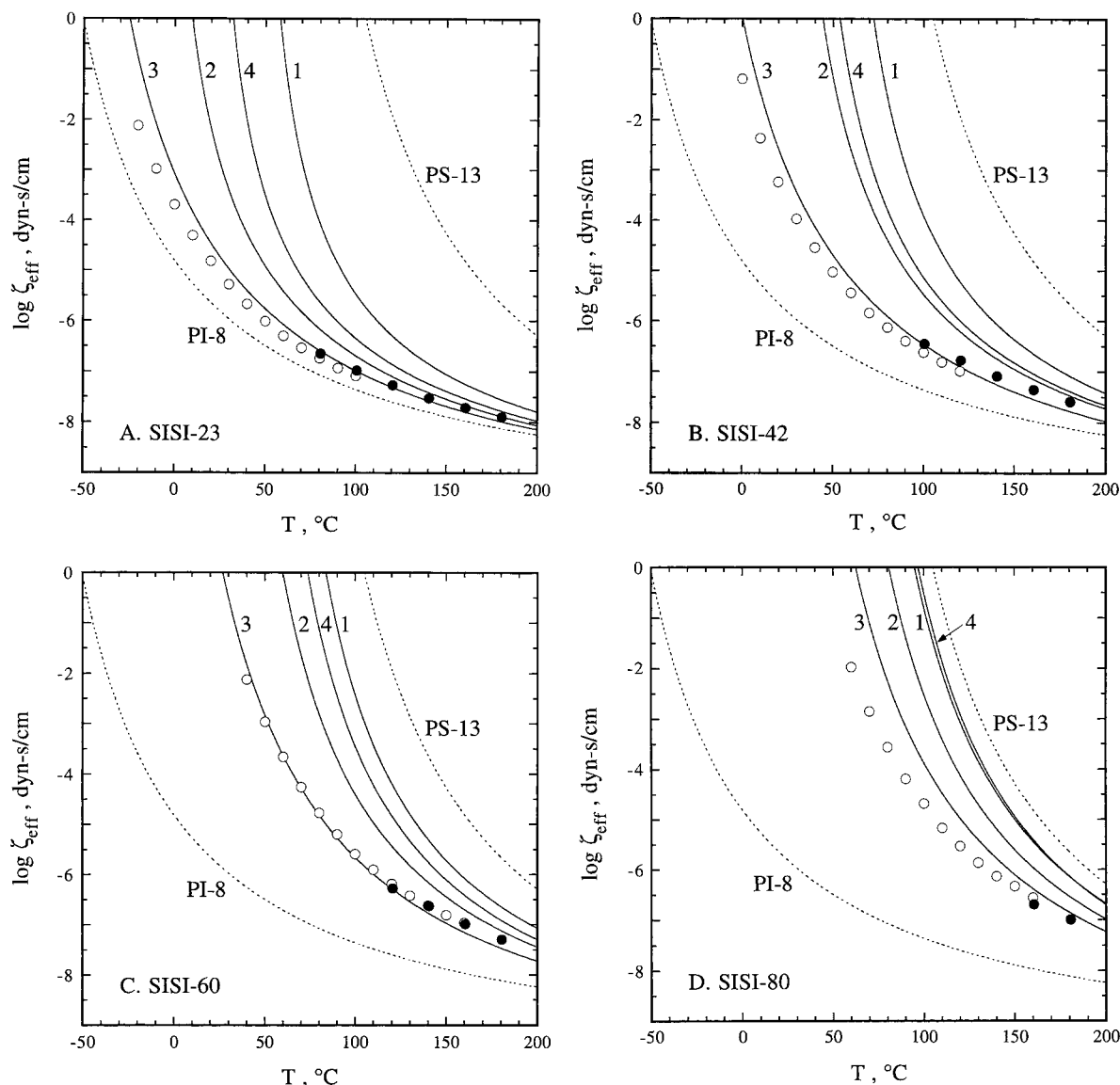


Figure 10. Effective monomeric friction factors as functions of temperature compared to the predictions of methods 1–4 (as defined in the text), for (A) SISI-23, (B) SISI-42, (C) SISI-60, and (D) SISI-80. The homopolymer fits from Figure 8 are included for reference.

These observations further highlight the need for information on the effective T_g of each component in the mixture, which apparently embodies most of the important physics behind ζ_{eff} . Values can be obtained through segmental relaxation time measurements (e.g., by NMR, dielectric relaxation, or depolarized light scattering). On the basis of data for miscible blends and the increase in $G''(T)$ peak dispersion, we expect the individual T_g 's could be up to ± 10 °C different from the measured T_g for each tetrablock. This feature has important implications for predicting $\zeta_{\text{eff}}(f, T)$. Specifically, since the difference in $T_g(\text{PS})$ and $T_g(\text{PI})$ is presumably related to the same balance of intra- and intermolecular constraints reflected in the monomeric friction factor, incorporation of a reasonable model for $T_g(f)$ of each component may provide a means (albeit indirect) to account for these effects in the mixing rule calculations.

Even with an understanding of $T_g(f)$ and correcting for the influence of local density, a quantitative description of $\zeta_{\text{eff}}(f, T)$ may not be possible with the simple approach outlined above because we have not considered the role of A–B interactions explicitly. That is, the

chemical identity of the local environment should also affect the friction factor, as reflected directly in $\zeta_A(f, T)$ and $\zeta_B(f, T)$. A promising approach to incorporating the effects of A–B interactions would be to exploit “cross terms” $\zeta_{A/B}(T)$ and $\zeta_{B/A}(T)$ that parametrize the friction experienced by one monomer in a pure matrix of the other; $\zeta_A(f, T)$ and $\zeta_B(f, T)$ would then be expressed as appropriate averages of the homopolymer and cross terms, and $\zeta_{\text{eff}}(f, T)$ calculated using a mixing rule that combines $\zeta_A(f, T)$ and $\zeta_B(f, T)$ rather than $\zeta_A^0(T)$ and $\zeta_B^0(T)$. The result, using the volume fraction-weighted geometric mean protocol in both steps, is

$$\log[\zeta_{\text{eff}}(f, T)] = f^2 \log[\zeta_A^0(T)] + f(1 - f) [\log[\zeta_{A/B}(T)] + \log[\zeta_{B/A}(T)]] + (1 - f)^2 \log[\zeta_B^0(T)] \quad (14)$$

The middle term could incorporate the thermodynamic barrier contribution postulated in association with eq 9. In this respect, $\zeta_{A/B}$ and $\zeta_{B/A}$ depend on χN , as one would intuitively expect. However, since $\zeta_{A/B}$ and $\zeta_{B/A}$ values are not available for immiscible systems such as PS/PI, the applicability of this mixing rule cannot

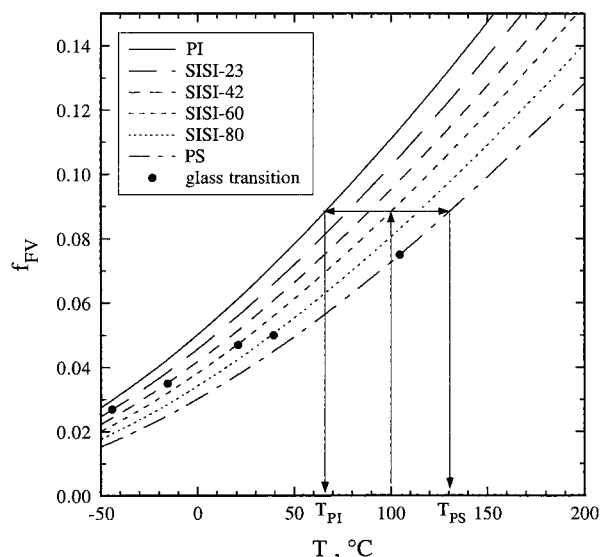


Figure 11. Fractional free volume as a function of temperature for the four tetrablocks and the two homopolymers, as predicted by the Sanchez–Lacombe equation of state. The determination of T_{PS} and T_{PI} , the temperatures at which the fractional free volume in the pure homopolymers equals that in a given tetrablock at temperature T , is also illustrated.

be tested here. Moreover, if used as a predictive tool, this framework would still require resolution of the issue of which matrix values (corresponding to different T_g definitions) to use as inputs.

Summary

The temperature dependence of the diffusivity and viscosity has been examined for four styrene–isoprene tetrablock copolymers of different compositions and styrene and isoprene homopolymers, all with approximately constant degrees of polymerization. The tetrablock copolymers were well above their respective order–disorder transitions, as determined from the temperature dependence of the SANS structure factors, and the structure factors were reasonably well-described by the Leibler/RPA approach. Glass transition temperatures were inferred from maxima in the temperature dependence of the dynamic loss modulus, G'' , and the resulting T_g values showed a slightly more pronounced composition dependence than that predicted by the Fox equation. Monomeric friction factors, $\zeta(T)$, were extracted via the Rouse model, and found to be equivalent between the two dynamic properties; for the tetrablocks, this ζ was termed ζ_{eff} , as there was no resolution of the (possibly different) contributions from styrene and isoprene segments. For all six materials, $\zeta(T)$ followed the standard WLF form, and at fixed temperature ζ increased strongly with styrene content, particularly on the styrene-rich side of the composition diagram. At constant $T - T_g$, however, ζ was only a slight function of composition, in marked contrast to some miscible blends that have been described in the literature; ζ consistently exceeded both ζ_{PS} and ζ_{PI} , but by well under an order of magnitude.

Several methods for estimating ζ_{eff} on the basis of the pure homopolymer values were considered. A volume fraction-weighted geometric mixing rule, analogous to a successful mixing rule for the viscosity of small molecule mixtures, did a reasonable job of predicting ζ_{eff} when combined with the composition-dependent T_g predicted by the Fox equation. Consequently, for this

system the prediction of ζ_{eff} largely reduces to the prediction of the effective T_g experienced by each component in the tetrablocks. A more elaborate free-volume-based approach, utilizing equation-of-state estimates of free volume, was markedly less successful, as were more naive approaches that did not address the effect of mixing on T_g directly. In general, one expects that the composition dependence of monomeric friction factors in homogeneous mixtures will incorporate interaction terms that are not known a priori, but in this particular system such interaction terms appear to be modest at best. In the next phase of this project, homopolymer tracer diffusion in the tetrablocks, dielectric relaxation, and depolarized light scattering will be employed to resolve the separate composition dependences of the styrene and isoprene friction factors.

Acknowledgment. This work was supported in part by the National Science Foundation, through Grant DMR-9528481 (T.P.L.), by the Center for Interfacial Engineering, an NSF-sponsored Engineering Research Center at the University of Minnesota, and by the NSF-REU Program (C.K.). We appreciate helpful discussions with G. Berry.

Appendix

Here we estimate the free volume of PS/PI mixtures as required for the “method 4” mixing rule described in the text. The fractional free volume is written in terms of a reduced density, $f_{FV} = 1 - \rho/\rho^*$, where ρ^* is the hard-core density that would be observed at absolute zero temperature, i.e., in the absence of free volume. ρ/ρ^* can be readily calculated as a function of f and T using an appropriate equation of state; we adopt one derived from the lattice-fluid theory of Sanchez and Lacombe.^{31,32}

The Sanchez–Lacombe equation of state for a polymer liquid, in the zero-pressure limit, is

$$\tilde{\rho}^2 + T[\ln(1 - \tilde{\rho}) + \tilde{\rho}] = 0 \quad (15)$$

where $\tilde{T} = T/T^*$, $\tilde{P} = P/P^*$, $\tilde{\rho} = \rho/\rho^*$, and T^* , P^* , and ρ^* are characteristic parameters. For a mixture, these parameters become functions of composition and the pure component T^* , P^* , and ρ^* values. The postulated combining rules are^{31,32}

$$T^* = P^* \left[\frac{\phi_A P_A^*}{T_A^*} + \frac{\phi_B P_B^*}{T_B^*} \right]^{-1} \quad (16)$$

$$P^* = \phi_A P_A^* + \phi_B P_B^* - \phi_A \phi_B \Delta P^* \quad (17)$$

$$\rho^* = \left[\frac{w_A}{\rho_A^*} + \frac{w_B}{\rho_B^*} \right]^{-1} \quad (18)$$

where w and ϕ are weight and volume fractions, respectively. ΔP^* is a “bare” binary interaction parameter, related to the change in cohesive energy density upon A–B exchange, that characterizes the direct energetic interactions between A and B monomers.

The equation of state parameters for PS and PI are reported in Table 5. Values for PS were taken directly from the literature.^{28,31,32} Values for PI were obtained as follows. First, specific volume vs temperature data (atmospheric pressure, $10 < T < 85$ °C) for un-cross-linked Hevea rubber³³ were fit using eq 16 to determine T^* and ρ^* . Next, values for the thermal expansion

Table 5. Sanchez–Lacombe Equation of State Parameters for Polystyrene (PS) and Polyisoprene (PI)

polymer	T^* , K	P^* , bar	ρ^* , g/cm ³
PS	735	3570	1.105
PI	618	4150	0.970

coefficient ($\alpha = 6.70 \times 10^{-4} \text{ K}^{-1}$) and the isothermal compressibility ($\beta = 5.15 \times 10^{-5} \text{ bar}^{-1}$) of PI at 25 °C³⁴ were combined with the measured density at 25 °C³³ to calculate P^* as

$$P^* = \frac{T\alpha}{\tilde{\rho}\beta} \quad (19)$$

ΔP^* was calculated by comparing the expression for the Flory–Huggins χ parameter derived from the Sanchez–Lacombe equation of state^{35,36}

$$\chi = \frac{V_0}{RT} [B^H - TB^S] \quad (20)$$

to the temperature dependence of χ (styrene–isoprene) reported for PS–PI copolymers¹⁹

$$\chi = \frac{33 \text{ K}}{T} - 0.0228 \quad (21)$$

where χ is defined using a styrene monomer for the reference volume ($v_0 = 99 \text{ cm}^3/\text{mol}$). The terms B^H and B^S represent enthalpic and noncombinatorial entropic contributions to χ . The Sanchez–Lacombe expression for the former is^{31,32,35,36}

$$B^H = \tilde{\rho} \Delta P^* + \left[\frac{P_A^*}{\phi_A} (\tilde{\rho}_A - \tilde{\rho}) + \frac{P_B^*}{\phi_B} (\tilde{\rho}_B - \tilde{\rho}) \right] \quad (22)$$

Assuming eqs 20 and 21 can be compared term by term, so that $(v_0/R)B^H = 33 \text{ K}$, we use eq 22 (with $\phi_{PS} \approx 0.5$, $T \approx 300 \text{ K}$, and pure component parameters from Table 5) to calculate ΔP^* in a self-consistent manner; i.e., we assume a value for ΔP^* , use eqs 16 and 17 to determine T^* for the mixture, calculate $\tilde{\rho}$ via eq 15 to input into eq 22, and iterate until ΔP^* from the B^H calculation converges. The final value is $\Delta P^* \approx 100 \text{ bar}$, which is the same order of magnitude as values reported for other immiscible monomer pairs (e.g., styrene/acrylonitrile).^{35,36}

The predicted temperature dependence of the fractional free volume of the tetrablocks and homopolymers is shown in Figure 11. Values at the measured T_g s are indicated by filled circles; it is apparent that the glass transition is far from an iso-fractional free volume state in this framework. An example of how these results are used in the method 4 calculation is depicted by the

arrows: to predict $\zeta_{\text{eff}}(\phi = 0.60, T = 100 \text{ °C})$, the appropriate homopolymer values to input into the mixing rule are $\zeta_{PI}(T_{PI})$ and $\zeta_{PS}(T_{PS})$.

References and Notes

- (1) Berry, G. C.; Fox, T. G. *Adv. Polym. Sci.* **1968**, *5*, 261.
- (2) Ferry, J. D. *Viscoelastic Properties of Polymers*, 3rd ed.; Wiley: New York, 1980.
- (3) Composto, R. J.; Kramer, E. J.; White, D. M. *Polymer* **1990**, *31*, 2320.
- (4) Kim, E.; Kramer, E. J.; Osby, J. O. *Macromolecules* **1995**, *28*, 1979.
- (5) Green, P. F.; Adolf, D. B.; Gilliom, L. R. *Macromolecules* **1991**, *24*, 3377.
- (6) Colby, R. H. *Polymer* **1989**, *30*, 1275.
- (7) Roovers, J.; Toporowski, P. M. *Macromolecules* **1992**, *25*, 1096, 3454.
- (8) Chung, G.-C.; Kornfield, J. A.; Smith, S. D. *Macromolecules* **1994**, *27*, 5729.
- (9) Leibler, L. *Macromolecules* **1980**, *13*, 1602.
- (10) Eastman, C. E.; Lodge, T. P. *Macromolecules* **1994**, *27*, 5591.
- (11) Faldi, A.; Tirrell, M.; Lodge, T. P. *Macromolecules* **1994**, *27*, 4176.
- (12) Stejskal, E. O.; Tanner, J. E. *J. Chem. Phys.* **1965**, *42*, 288.
- (13) von Meerwall, E.; Grigsby, J.; Tomich, D.; Van Antwerp, R. *J. Polym. Sci., Polym. Phys. Ed.* **1982**, *20*, 1037.
- (14) von Meerwall, E. D.; Ferguson, R. D. *Comput. Phys. Commun.* **1981**, *21*, 421.
- (15) von Meerwall, E.; Kamat, M. *J. Magn. Reson.* **1989**, *83*, 309.
- (16) Higgins, J. S.; Benoit, H. C. *Polymers and Neutron Scattering*; Clarendon Press: Oxford, England, 1994.
- (17) Almdal, K.; Rosedale, J. H.; Bates, F. S.; Wignall, G. D.; Fredrickson, G. H. *Phys. Rev. Lett.* **1990**, *65*, 1112.
- (18) Bates, F. S.; Fredrickson, G. H. *Annu. Rev. Phys. Chem.* **1990**, *41*, 525.
- (19) Lodge, T. P.; Pan, C.; Jin, X.; Liu, Z.; Zhao, J.; Maurer, W. W.; Bates, F. S. *J. Polym. Sci., Polym. Phys. Ed.* **1995**, *33*, 2289.
- (20) Fox, T. G. *Bull. Am. Phys. Soc.* **1956**, *1*, 123.
- (21) Gordon, M.; Taylor, J. S. *J. Appl. Chem.* **1952**, *2*, 1.
- (22) Couchman, P. R. *Macromolecules* **1978**, *11*, 1156.
- (23) Hamersky, M. W.; Tirrell, M.; Lodge, T. P. *J. Polym. Sci., Polym. Phys. Ed.* **1996**, *34*, 2899.
- (24) Gisser, D. J.; Ediger, M. D. *Macromolecules* **1992**, *25*, 1284.
- (25) Friedman, E. M.; Porter, R. S. *Trans. Soc. Rheol.* **1975**, *19*, 493.
- (26) Bloomfield, V. A.; Dewan, R. K. *J. Phys. Chem.* **1971**, *75*, 3113.
- (27) Arrhenius, S. *Z. Phys. Chem.* **1887**, *1*, 285.
- (28) Kow, C.; Morton, M.; Fetters, L. J.; Hadjichristidis, N. *Rubber Chem. Technol.* **1982**, *55*, 245.
- (29) O'Driscoll, K.; Sanayei, R. A. *Macromolecules* **1991**, *24*, 4479.
- (30) Doolittle, A. K. *The Technology of Solvents and Plasticizers*; Wiley: New York, 1954.
- (31) Sanchez, I. C.; Lacombe, R. H. *J. Polym. Sci., Polym. Lett.* **1977**, *15*, 71.
- (32) Sanchez, I. C.; Lacombe, R. H. *Macromolecules* **1978**, *11*, 1145.
- (33) Scott, A. H. *J. Res. Natl. Bur. Stand.* **1935**, *14*, 99.
- (34) *Polymer Handbook*, 3rd ed.; Brandrup, J., Immergut, E. H., Eds.; John Wiley & Sons: New York, 1989.
- (35) Kim, C. K.; Paul, D. R. *Polymer* **1992**, *33*, 1630.
- (36) Gan, P. P.; Paul, D. R.; Padwa, A. R. *Polymer* **1994**, *35*, 1487.

MA971797Q